ANTICANCER RESEARCH *42*: 471-482 (2022)
doi:10.21873/anticanres.15505

Blockade of GRP78 Translocation to the Cell Surface by HDAC6 Inhibition Suppresses Proliferation of Cholangiocarcinoma Cells

CHORONG KIM[1], SEONMIN LEE[1], DANBEE KIM[1], DA SOL LEE[1], EUNJUNG LEE[1], CHANGHOON YOO[2] and KYU-PYO KIM[2]

[1]*Asan Institute for Life Sciences, Asan Medical Center, Seoul, Republic of Korea;*
[2]*Department of Oncology, Asan Medical Center, University of Ulsan College of Medicine, Seoul, Republic of Korea*

Abstract. *Background/Aim: HDAC6, a cytoplasmic localized deacetylase, is a positive regulator of cancer progression via modification of various substrates. We evaluated how the interaction between HDAC6 and glucose regulatory protein 78 (GRP78) affects the growth of cholangiocarcinoma (CCA). Materials and Methods: The anti-tumor effects of ACY-1215, an HDAC6 specific inhibitor, in CCA cell lines were analyzed by cell viability assay, western blotting, flow cytometry, co-immunoprecipitation, and biotinylation assays. In vivo effects of ACY-1215 were evaluated in a xenograft model using CCA cell line TFK-1. Results: ACY-1215 increased the acetyl-form of GRP78 by approximately 50% compared to control, which impaired the translocation of GRP78 to the plasma membrane by 50% through alteration of cellular proliferative signaling via PI3K/AKT. Furthermore, ACY-1215 suppressed tumor growth by 50% compared to vehicle control in a CCA xenograft model. Conclusion: Increase in GRP78 acetylation by HDAC6 inhibition suppressed GRP78 translocation to the cell surface, which inhibited proliferation and promoted apoptosis in CCA.*

Cholangiocarcinoma (CCA) is a malignancy arising from the epithelial cells lining the bile ductal tree. Although surgical resection is the preferred curative treatment of CCA, it is restricted to patients with early stage-CCA. Based on the ABC-02 phase III clinical study, gemcitabine and cisplatin are used as the standard care for patients with advanced biliary tract cancer (BTC). However, significant positive therapeutic outcomes have not been achieved (1).

Correspondence to: Kyu-Pyo Kim, Department of Oncology, Asan Medical Center, University of Ulsan College of Medicine, 88, Olympic-ro 43-gil, Songpa-gu, Seoul 05505, Republic of Korea. Tel: +82 230105913, Fax: +82 220454046, e-mail: kkp1122@amc.seoul.kr

Key Words: HDAC6, cholangiocarcinoma, GRP78, acetylation, ACY-1215.

In recent years, histone deacetylases (HDACs), which catalyze the deacetylation of proteins, have become an emerging therapeutic target for CCA. HDACs contribute to the proliferation, invasion, metastasis, migration, and chemoresistance of CCA through epigenetic regulation. These effects are suppressed by pan-HDAC inhibitors, including vorinostat, trichostatin A, and CG200745 (2-4). Among the various HDACs, HDAC6 has been highlighted as a cancer therapy target. Gradilone et al. have reported that HDAC6 is over-expressed in tissues from patients with CCA, and it induces tumorigenesis by regulating ciliary function in CCA (5). In addition, HDAC6 is specifically localized in the cytosol, and modulation of its substrates including α-tubulin, heat shock protein 90, and glucose regulatory protein 78 (GRP78) is involved in cancer biology (6, 7).

GRP78 has been found to be upregulated in various cancer types. Due to the rapid growth of cancer cells and limited vascularization, the tumor environment undergoes stress conditions (*e.g.*, hypoxia, nutrient deprivation, and acidosis), which lead to prolonged endoplasmic reticulum (ER) stress in cancer cells. To alleviate ER stress and maintain ER homeostasis, GRP78 expression is maintained at high basal levels. Although it was first identified in the ER lumen, recent studies have demonstrated that GRP78 is ubiquitous in the cell and its roles are different according to subcellular locations (8-10). A cytoplasmic isoform of GRP78 (GRP78va) is over-expressed in leukemia cells and contributes to their survival (11). GRP78 in the nuclei plays a role in blocking DNA-damage-induced apoptosis in hepatoma cells (8, 12). Furthermore, the GRP78 secreted by colon cancer and HCC cells promotes cell proliferation (13, 14).

Interestingly, several studies have shown that GRP78 is translocated to the plasma membrane in various cancer types. Cell surface GRP78 (cs-GRP78) has important roles in cell proliferation, metastasis, migration, invasion, apoptosis resistance, and chemoresistance in many types of cancer cells (15, 16). The cs-GRP78 is an α2-macroglobulin signaling

receptor, transmitting signals that increase the motility of prostate cancer cells (17). Moreover, a specific anti-GRP78 antibody suppressed the function of cs-GRP78 and inhibited breast cancer cell proliferation and migration (18).

So far, the role of HDAC6 and GRP78 in tumor biology has been described in various cancers (7, 19); however, the relationship between HDAC6 and GRP78 is still unclear in CCA. In this study, we identified the role of HDAC6 and GRP78 in CCA and validated HDAC6 inhibition as a target for treatment of CCA.

Materials and Methods

Cell lines and culture. The human CCA cell lines SNU-245, SNU-308, and SNU-1196 were purchased from the Korean Cell Line Bank (Seoul, Republic of Korea). The human CCA cell lines SSP-25 and TFK-1 were obtained from Asan Preclinical Evaluation center for cancer therapeutiX (Seoul, Republic of Korea). The cells were cultured in RPMI-1640 medium (Gibco, Grand Island, NY, USA) supplemented with 10% fetal bovine serum (WELGENE, Gyeongsan, Republic of Korea) and 1% penicillin/streptomycin (Gibco). The human cholangiocyte cell line MMNK-1 was obtained from the JCRB Cell Bank, National Institute of Biomedical Innovation, Health, and Nutrition (Osaka, Japan). The cells were cultured in Dulbecco's Modified Eagle Medium (Gibco) containing 5% fetal bovine serum and 1% penicillin/streptomycin. All the cells were maintained in an incubator at 37˚C, 5% CO_2.

Co-Immunoprecipitation. Cells were lysed in Cell Extraction Buffer (Invitrogen, Camarillo, CA, USA) containing a protease inhibitor cocktail (Roche, Mannheim, Germany). Then, 1 mg protein from the whole-cell lysates was precleared with 30 μl of Pierce Protein A/G agarose (Thermo Scientific, Rockford, IL, USA) in a rotator for 3 h at 4˚C, followed by centrifugation at 700 × *g* for 5 min at 4˚C. The supernatant was mixed with 2 μg of anti-GRP78 antibody (ab21685; Abcam, Cambridge, UK) or anti-Acetylated-Lysine antibody (#9441; Cell Signaling, Danvers, MA, USA) and incubated in a rotator at 4˚C overnight. Then, 50 μl of Pierce Protein A/G agarose was added, and the sample was further incubated in a rotator for 6 h at 4˚C. The beads were pulled down by centrifugation and washed with Cell Extraction Buffer 5 times. The complex-bound beads were mixed with 100 μl of 4× LDS Sample Buffer (Invitrogen), followed by boiling for 5 min at 95˚C and centrifugation at 700 × *g* for 5 min.

Cell surface protein biotinylation assay. After removal of the used medium, the cells were washed with ice-cold PBS twice. EZ-link Sulfo-NHS-LC-Biotin (Thermo Scientific) in ice-cold PBS at 0.25 mg/ml was applied to couple the surface protein with biotin (10 ml/100 mm plate), and the plate was gently shaken for 30 min at 4˚C. To stop the biotinylation reaction, quenching solution (Thermo Scientific) was added, and the plate was tipped back and forth. The cells were scraped into the solution and transferred to a conical tube. Then, the cells were rinsed with ice-cold TBS twice and lysed in lysis buffer (Thermo Scientific) containing a protease inhibitor cocktail (Roche). During incubation, the cells were sonicated using five 1-s bursts at 1.5-low power to enhance the solubilization efficiency. The lysates were treated with NeutrAvidin Agarose (Thermo Scientific) for 1 h at room temperature to purify the surface proteins. The beads were then washed with washing buffer (Thermo Scientific) containing a protease inhibitor cocktail and centrifuged at 1,000 × *g* for 1 min 4 times. Then, 400 μl of 4× LDS Sample Buffer (Invitrogen) was added, followed by heating for 5 min at 95˚C. The surface proteins were collected by centrifuging at 1,000 × *g* for 2 min.

Flow cytometry analysis. The expression levels of cell surface GRP78 were detected by flow cytometry. TFK-1 cells were harvested at a density of 1×10^6 cells/ml in cell staining buffer plus 0.5% BSA (Gibco) in PBS (Thermo Scientific). To reduce non-specific immunofluorescence staining, the cells were mixed with 1 μg of purified human Fc receptor binding inhibitor solution (Invitrogen), followed by incubation with an anti-GRP78 antibody (ab188878; Abcam) or rabbit IgG polyclonal antibody (ab171870; Abcam) for 1 h at 4˚C. The cells were gently mixed every 10 min during this procedure. After centrifugation at 400 × *g* for 5 min at 4˚C, the cells were washed with cell staining buffer twice and incubated with goat anti-rabbit IgG antibody (A21070; Life Technologies, USA) for 30 min at 4˚C in the dark. The cells were gently mixed every 10 min during this procedure, followed by resuspension in 200~300 μl of cell staining buffer. The cells were then analyzed using a FACS Canto II flow cytometer (BD Biosciences, San Jose, CA, USA) and FlowJo V10 software (FlowJo, USA). The FACS Canto II was operated by the Flow Cytometry Core Facility, Research Development Support Center, Asan Medical Center.

Apoptosis assay. Annexin V/Propidium Iodide (PI) double staining was performed for apoptosis analysis. After treatment with ACY-1215 (MedChemExpress, Monmouth Junction, NJ, USA), 1 × 106 cells were rinsed with PBS, followed by centrifugation at 300 × *g* for 10 min at 4˚C. The cells were washed with 1 ml of 1× binding buffer (Miltenyi Biotec, Bergisch Gladbach, Germany) twice and resuspended in 100 μl of 1× binding buffer, followed by staining with 10 μl of Annexin V-FITC (Miltenyi Biotec) for 30 min at room temperature in the dark. Then, 1 ml of 1× binding buffer was added to the cells, followed by centrifugation at 300 × *g* for 10 min at 4˚C. Subsequently, the cells were resuspended in 500 μl of 1× binding buffer and mixed with 5 μl of PI (Miltenyi Biotec). The cells were incubated for a further 15 min at room temperature in the dark. The cells were then analyzed using a FACS Canto II flow cytometer (BD Biosciences) and FlowJo V10 software (FlowJo). The FACS Canto II was operated by the Flow Cytometry Core Facility, Research Development Support Center, Asan Medical Center.

Western blotting. Whole-cell lysates were prepared by heating in 4× LDS Sample Buffer (Invitrogen). The proteins were loaded into the wells of NuPAGE™ 4-12% Bis-Tris Protein Gels (Invitrogen) and separated using SDS-PAGE in MES SDS Running Buffer (Invitrogen). The proteins separated according to their molecular weight were transferred onto polyvinylidene difluoride membranes (Invitrogen) in transfer buffer (Novex, Carlsbad, CA, USA). The membranes were blocked with 5% skim milk or BSA in Tris-buffered saline containing Tween-20 (TBST) (iNtRON Biotechnology, Seongnam, Republic of Korea) on an orbital shaker for 1 h at room temperature. After incubation with primary antibodies overnight at 4˚C, the membranes were rinsed with TBST 3 times and then incubated with horseradish peroxidase-conjugated secondary antibodies (Cell Signaling) for 1 h at room temperature on an orbital shaker. The membranes were rinsed with TBST thrice for 10 min, followed by treatment with SuperSignal West Femto Stable Peroxide

Buffer (Thermo Scientific) to enhance the signals and then detected by using a Chemiluminescence Imaging System (ATTO, Japan). The sources of the antibodies are listed below. Antibodies against α-tubulin (#2144), acetylated-lysine (#9441), acetyl-α-tubulin Lys40 (#5335), Akt (#4691), Bad (#9268), cleaved PARP (#5625), HDAC6 (#7558), phospho-Akt Ser473 (#4060), phospho-Akt Thr308 (#9275), phospho-bad Ser112 (#9291), phospho-bad Ser136 (#4366), and ubiquitin (#3936) were from Cell Signaling. β-actin (A5441) was from Sigma-Aldrich (Saint Louis, MO, USA). PERK (sc-377400) was from Santa Cruz Biotechnology (Santa Cruz, CA, USA). Annexin-2/ANXA2 (ab41803), GRP78 (ab21685), and p-PERK Thr982 (ab192591) were from Abcam (UK). The numerical intensity of the bands was calculated using the program ImageJ v1.52a.

Transfection. The day before transfection, TFK-1 cells were seeded into 24-well plates (4×10^4 cells/well) or 6-well plates (2×10^5 cells/well). For knockdown of *HDAC6* gene, ON-TARGETplus Human HDAC6 (10013) siRNA - SMARTpool as well as ON-TARGETplus Non-targeting Control Pool (Dharmacon, Lafayette, CO, USA) were used. In this study, we used a final siRNA concentration of 10 nM. Transfection was performed using DharmaFECT 1 Transfection Reagent (Dharmacon) according to the manufacturer's instructions.

Cell viability assay and IC_{50} assay. The cells were seeded in triplicate at a density of 2×10^3 cells in 50 μl per well of a 96-well plate and incubated for 24 h at 37˚C. The ACY-1215 (MedChemExpress), gemcitabine, cisplatin, and oxaliplatin (Sigma-Aldrich) were diluted with growth medium to 2× of their final concentration, followed by the addition of 50 μl of each drug solution to the cells. Then, 20 μl of CellTiter-Glo® Luminescent Cell Viability Assay solution (Promega, Madison, WI, USA) in 100 μl of culture medium was added into each well of the 96-well plate containing the cells. The contents were mixed for 2 min on an orbital shaker for cell lysis, followed by incubation at room temperature for 10 min to stabilize the luminescent signal. The solution (100 μl/well) was transferred to white 96-well plates, and then luminescence was read with a PerkinElmer VICTOR X2. For cell growth analysis, the number of cells was normalized to the negative control (vehicle). For the half-maximal inhibitory concentration (IC_{50}), the cell viability data were plotted as the percentage inhibition against the log value of the concentrations of the drug. The IC_{50} was determined using GraphPad Prism v5.01 (GraphPad Software).

For assessing transfected cell growth, the total number of cells was measured every 24 h for 5 days. At each stage, the cells were trypsinized, stained with trypan blue (Gibco) and the live cells were counted using a hemocytometer (Reichert-Jung, Cambridge instruments Inc., Buffalo, NY, USA).

Xenografts. The TFK-1 cells (5×10^6) were subcutaneously injected into the right flanks of 5-week-old BALB/c male nude mice (Central Laboratory Animal Inc., Republic of Korea). When the tumors reached approximately 80 to 150 mm^3, the animals were randomized into vehicle control and ACY-1215 treatment groups of 7 mice each. The ACY-1215 (50 mg/kg) was diluted in 5% DMSO (Sigma-Aldrich)/45% PEG-400 (Daejung, Republic of Korea)/50% ddH_2O buffer and administered intraperitoneally 5 days a week for 3 weeks. The tumor size was measured twice a week and calculated by the formula (length × width × width)/2. After completing the last treatment, the mice were euthanized, and the tumors were harvested for analysis. The detailed information of the animal study was described in the ARRIVE guidelines 2.0. All experiments were approved by the Institutional Animal Care and Use Committee of the Asan Institute for Life Science.

Immunohistochemistry. The tumor tissues embedded in paraffin were deparaffinized using EZ Prep (Roche), and then rinsed with reaction buffer [Tris buffer (pH 7.6)] and treated with Cell Conditioner containing Tris/Borate/EDTA buffer (pH 8.4) for 60 min at 100˚C. Then, the sections were incubated with 3% Ultraview peroxidase inhibitor (Roche) for 4 min at 37˚C to block the innate hydroperoxidases. The sections were incubated with anti-acetyl-α-tubulin Lys40 antibody (#5335; Cell signaling) and anti-Ki-67 antibody (#9027; Cell signaling) for 36 min at 37˚C. After washing with reaction buffer, the sections were further incubated for 1 h with DISCOVERY UltraMap anti-Rb HRP antibody (Roche) for 16 min at 37˚C, and then stained using an Ultra View Universal DAB Detection Kit (Roche). Finally, the sections were washed with reaction buffer and stained with hematoxylin (Roche). The images on the slides were visualized with an Olympus BX40 light microscope (Olympus, Japan) at ×40 magnification.

Statistical analysis. Statistical analysis was performed using two-tailed Student's *t*-tests with GraphPad Prism 5 software (GraphPad, San Diego, CA, USA). A value of $p<0.05$ was considered to be statistically significant. Data are presented as mean±SEM.

Results

The CCA cell lines showed high sensitivity to the HDAC6 inhibitor. To check their sensitivity to ACY-1215, the available oral HDAC6 inhibitor, its half-maximal inhibitory concentration (IC_{50}) values were defined in a normal bile ductal cell line, MMNK-1, and various CCA cell lines including SNU-245, SNU-308, SNU-1196, SSP-25, and TFK-1. All CCA cell lines were more sensitive to ACY-1215 than MMNK-1 (Figure 1A). Then, to confirm the inhibitory effect of ACY-1215 on HDAC6 activity, the level of acetylation on α-tubulin was evaluated *via* western blot. High levels of acetylated α-tubulin were detected in the ACY-1215 treatment group, indicating ACY-1215 effectively inhibited HDAC6 activity. However, ACY-1215 did not affect HDAC6 expression (Figure 1B). In particular, among the CCA cell lines, the IC_{50} value of TFK-1 (IC_{50}=11.62 μM) was approximately 6-fold lower than that of MMNK-1 (IC_{50}=71.47 μM). These results indicated that the CCA cell lines had higher sensitivity to ACY-1215 than did the normal bile ductal cell line.

HDAC6 inhibition resulted in apoptotic cell death in CCA cell lines. To compare HDAC6-targeted therapy using ACY-1215 and established cytotoxic chemotherapy for CCA cell line, the TFK-1 cells were treated for 24 h with gemcitabine, cisplatin, or oxaliplatin, or ACY-1215. The cisplatin and oxaliplatin showed 20~30% cell death efficacy. Unlike cisplatin and oxaliplatin, gemcitabine did not induce cell death. However,

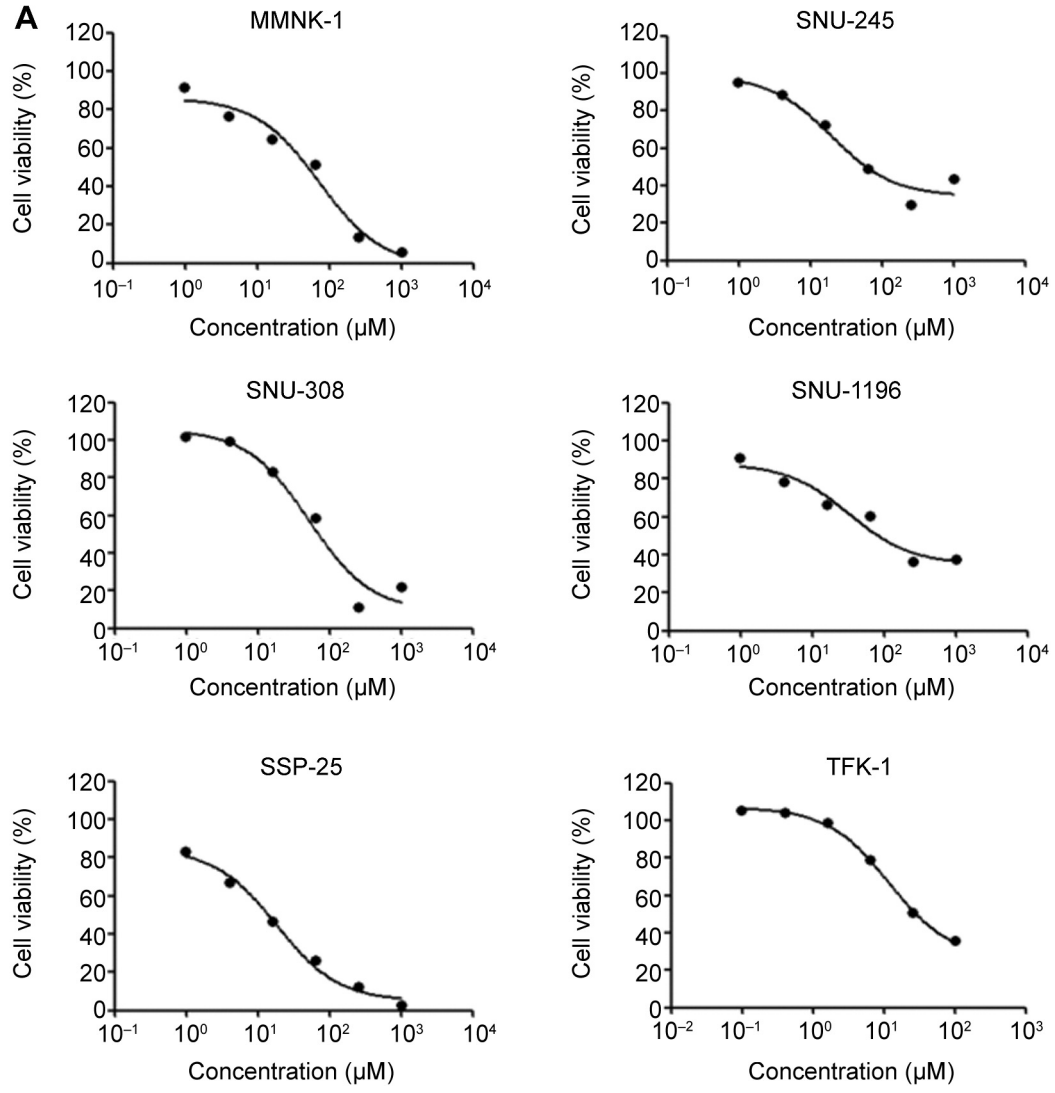

Cell Lines	MMNK-1	SNU-245	SNU-308	SNU-1196	SSP-25	TFK-1
IC_{50} (μM)	71.47	19.35	51.15	32.51	17.96	11.62

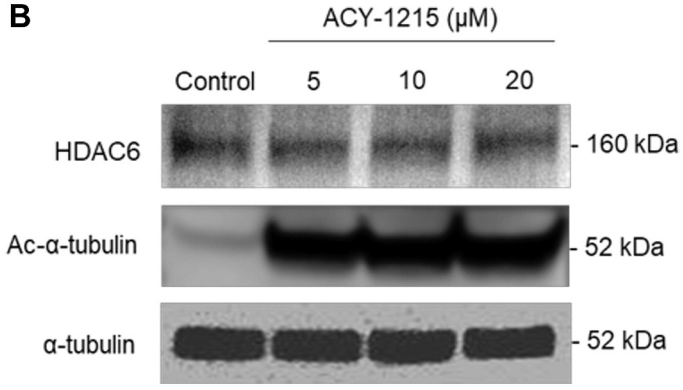

Figure 1. *Cholangiocarcinoma (CCA) cell lines have high sensitivity to HDAC6 inhibitor. (A) IC_{50} curve and table of ACY-1215, an HDAC6 inhibitor, in normal bile ductal cell line (MMNK-1), two extrahepatic CCA (SNU-245, TFK-1), gallbladder adenocarcinoma (SNU-308), and two intrahepatic CCA cell lines (SNU-1196, SSP-25). Cell viability was analyzed by CellTiter-Glo assay. (B) TFK-1 cells were treated with ACY-1215 at the indicated concentrations (5, 10 and 20 μM) for 24 h. HDAC6, acetyl-α-tubulin and α-tubulin were detected by western blot. All experiments were performed three times.*

ACY-1215 showed 50% viability (Figure 2A). Furthermore, the effect of ACY-1215 on cell viability occurred in a dose-dependent manner (Figure 2B). Besides, morphological changes were also induced by ACY-1215 (Figure 2C).

We next determine whether the death of TFK-1 cells induced by ACY-1215 is related to apoptosis. The numbers of both early (Q4) and late (Q2) apoptotic cells were increased after treatment with ACY-1215 at 20 μM (25.6%) compared with the untreated cells (6.9%). The numbers of early apoptotic cells significantly increased in a dose-dependent manner (Figure 2D). Western blotting data showed up-regulated cleaved PARP protein following ACY-1215 treatment (Figure 2E). Taken together, these findings suggested that ACY-1215 induces apoptotic cell death in the CCA cell line.

The novel role of GRP78 in the apoptosis signaling cascade upon HDAC6 inhibition. Our observations showed that HDAC6 inhibition led to apoptosis of the CCA cell line. We next sought to determine how HDAC6 inhibition by ACY-1215 induces apoptosis. A previous investigation reported that HDAC6 induced ER stress (20). First, the level of acetyl-α-tubulin was increased under ACY-1215 treatment, indicating the effective inhibition of HDAC6 activity by ACY-1215. Next, GRP78 expression was up-regulated two-fold at the highest dose of ACY-1215 (Figure 3A). The level of phospho-PERK (its active form), ER-stress regulator, was also increased under ACY-1215 treatment (Figure 3B). However, the accumulation of ubiquitinated proteins, a surrogate feature of ER stress, was not observed following ACY-1215 treatment (Figure 3C). These data suggested that GRP78 has a distinct role in the apoptosis signaling cascade that is independent of ER stress under the HDAC6 inhibition condition induced by ACY-1215.

HDAC6 inhibition suppressed the translocation of GRP78 to the cell surface via the accumulation of acetylation on GRP78. Several reports have demonstrated that GRP78 is translocated from the ER to the cell plasma membrane under ER stress in various types of cancer, including breast cancer, colorectal cancer, and prostate cancer (18, 21, 22). Accordingly, we checked whether GRP78 was located on the plasma membrane in CCA and whether HDAC6 inhibition by ACY-1215 had any effect on the localization of GRP78. To test these, we treated TFK-1 cells with ACY-1215 and measured cs-GRP78 by FACS as well as by biotinylation assay. Compared with untreated cells, the density of GRP78 protein located on the plasma membrane was reduced by approximately 50% after treatment with ACY-1215 (Figure 4A). Consistent with the biotinylation result, the level of GRP78 protein on the cell surface was reduced by approximately 36% after ACY-1215 treatment (Figure 4B).

We presumed that blockade of GRP78 translocation to the plasma membrane might be induced by the accumulation of acetylation on GRP78 by inhibition of HDAC6 activity. First, we checked whether the total amount of GRP78 was increased by ACY-1215 treatment (Figure 4C top). Next, we checked the level of acetyl-lysine on GRP78 by immunoprecipitation. The level of acetyl-lysine was increased approximately 2-fold under ACY-1215 treatment (Figure 4C middle, bottom). Taken together, ACY-1215 leads to the accumulation of acetylation on GRP78 through HDAC6 inhibition, which results in decreased GRP78 expression on the cell membrane.

Absence of cell surface GRP78 induced by ACY-1215 promoted apoptosis via AKT/Bad signaling. GRP78 located on the cell surface promotes cancer cell proliferation *via* PI3K/AKT signaling (16, 18) and drives apoptosis (8). First, we investigated AKT signaling under the condition of lacking cell surface GRP78 using ACY-1215. Following this treatment, the phosphorylation level of Ser473 on AKT, a survival signal, was sharply decreased even at the lower concentrations of ACY-1215 (Figure 4D). On the other hand, the phosphorylation level of Thr308 on AKT, blocking the signal of apoptosis *via* BAD phosphorylation, was also decreased in the cells exposed to ACY-1215 (Figure 4E). Moreover, the phosphorylation of Bad on both Ser112 and Ser136 decreased in the cells exposed to ACY-1215 compared with untreated cells (Figure 4E). These results indicate that lacking cell surface GRP78 induced by HDAC6 inhibition by ACY-1215 regulates proliferation and apoptosis *via* AKT/Bad signaling in CCA.

CCA cell growth was suppressed by silencing HDAC6. Since we confirmed the pharmaceutically anti-tumor effect of ACY-1215 *via* blocking GRP78 translocation to the cell surface, we next checked the biological role of HDAC6 knockdown on the growth of CCA cell line. In comparison with a scrambled siRNA-treated group, HDAC6 expression was markedly down-regulated in HDAC6 siRNA-treated group (Figure 5A). Moreover, we also assessed the function of HDAC6 in cs-GRP78 expression in the CCA cell line. HDAC6 siRNA markedly decreased the GRP78 located on the plasma membrane by approximately 3.1-fold in comparison with scrambled siRNA (Figure 5B). To investigate whether the knockdown of HDAC6 affects AKT signaling, we examined the activation state of AKT/BAD signaling pathways. Consistent with our study on ACY-1215, the phosphorylation level of the serines at 473 and threonines at 308 on AKT decreased in the cells after HDAC6 knockdown (Figure 5C). Knockdown of HDAC6 led to the down-regulation of proliferative signaling and up-regulation of apoptosis. HDAC6 knockdown significantly inhibited the cell growth rate of TFK-1 cells by 20.6% and 23.4%, at 48 and 72 h, respectively (Figure 5D). Our findings demonstrated that HDAC6 plays a role in CCA cell growth through AKT signalling.

HDAC6 inhibition suppressed tumor growth in a CCA xenograft model. To validate the therapeutic effects of ACY-1215 *in vivo*,

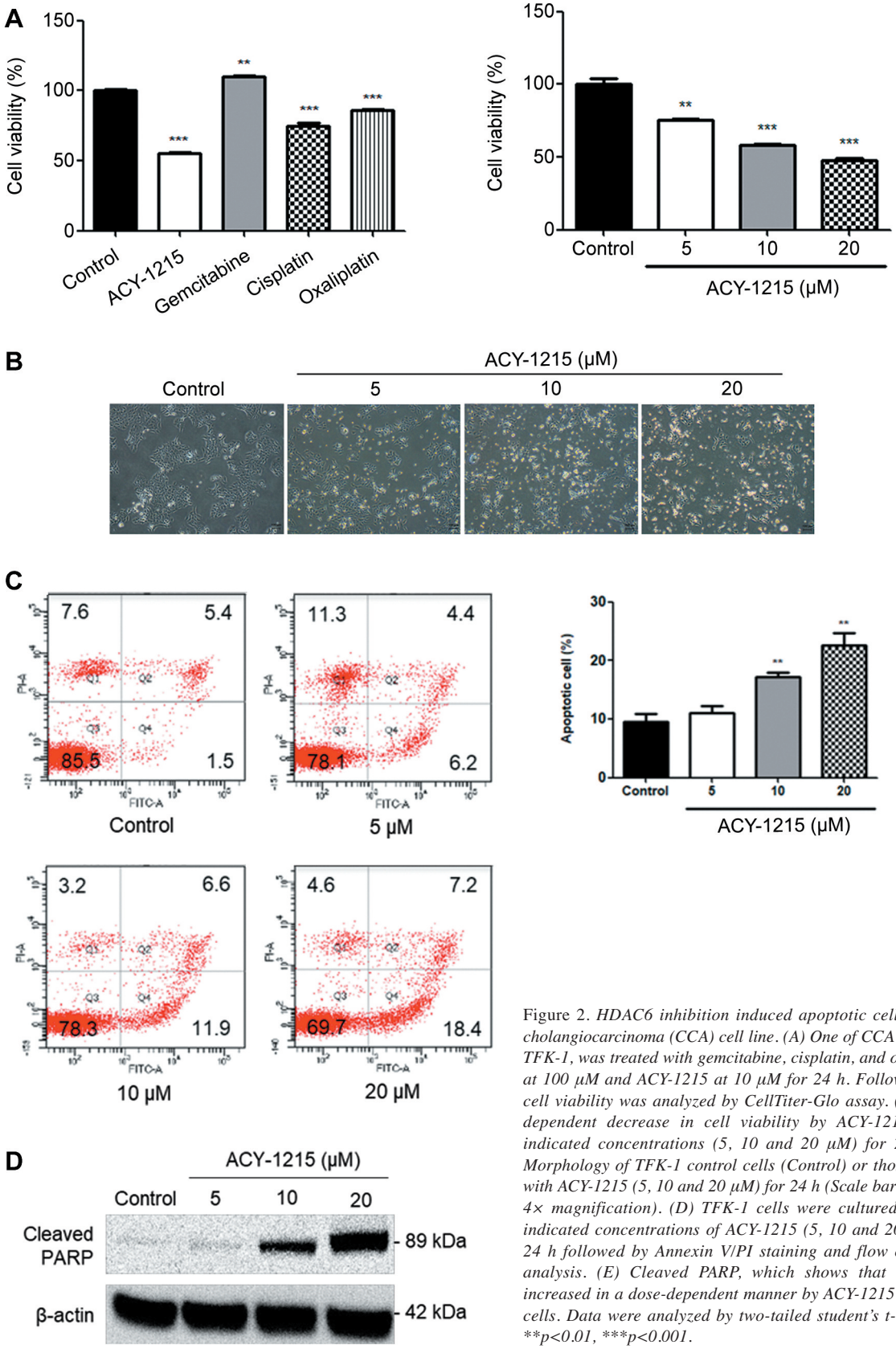

Figure 2. *HDAC6 inhibition induced apoptotic cell death in cholangiocarcinoma (CCA) cell line. (A) One of CCA cell lines, TFK-1, was treated with gemcitabine, cisplatin, and oxaliplatin at 100 μM and ACY-1215 at 10 μM for 24 h. Following that, cell viability was analyzed by CellTiter-Glo assay. (B) Dose-dependent decrease in cell viability by ACY-1215 at the indicated concentrations (5, 10 and 20 μM) for 24 h. (C) Morphology of TFK-1 control cells (Control) or those treated with ACY-1215 (5, 10 and 20 μM) for 24 h (Scale bar=100 μm, 4× magnification). (D) TFK-1 cells were cultured with the indicated concentrations of ACY-1215 (5, 10 and 20 μM) for 24 h followed by Annexin V/PI staining and flow cytometry analysis. (E) Cleaved PARP, which shows that apoptosis increased in a dose-dependent manner by ACY-1215 in TFK-1 cells. Data were analyzed by two-tailed student's t-test, n=3. **p<0.01, ***p<0.001.*

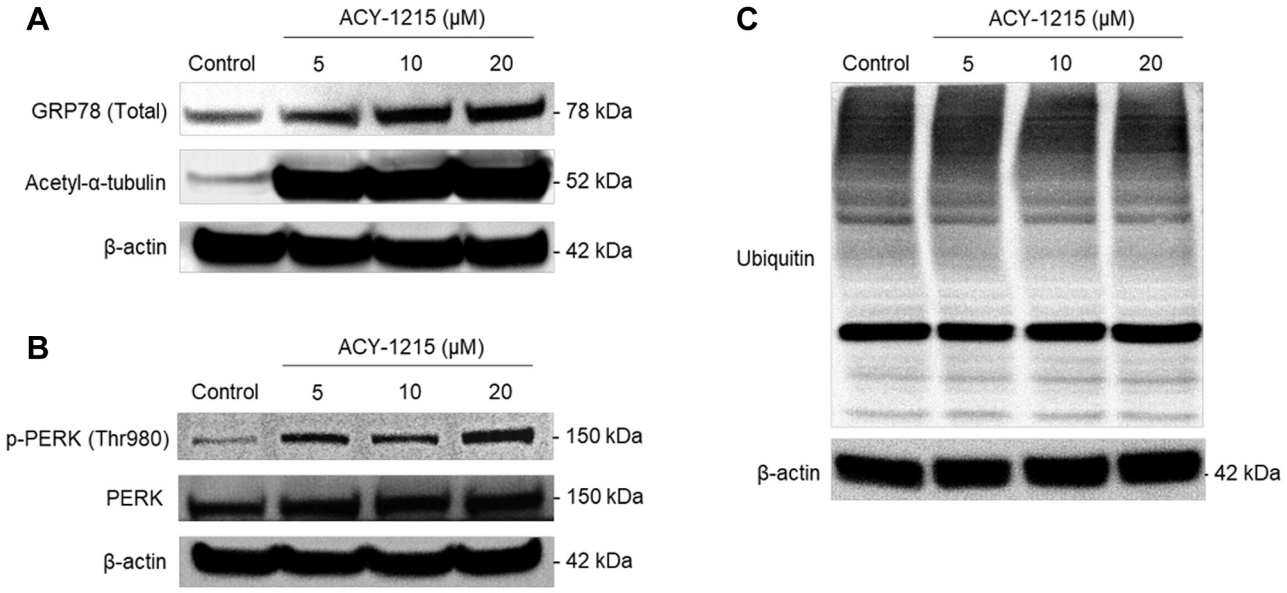

Figure 3. *HDAC6 inhibition increases endoplasmic reticulum (ER) stress but not ubiquitinated proteins. (A) Translational induction of GRP78 after treatment with ACY-1215 at the indicated concentrations (5, 10 and 20 μM) for 24 h. Acetyl-α-tubulin indicates the drug effect of ACY-1215. (B) Immunoblots of p-PERK (Thr980), PERK in TFK-1 lysates from cells treated with ACY-1215 (5, 10 and 20 μM). p-PERK (Thr980) serves as a marker for ER stress activation. (C) Ubiquitinated protein levels did not increase, although ER stress was induced by ACY-1215. The data shown here are representative of three independent experiments.*

we generated a CCA xenograft model using TFK-1 cells. The group treated with ACY-1215 showed a statistically significant tumor growth inhibition by 46% compared to vehicle control at day 76 (Figure 6A-D). The body weight changes of the animals indicated that toxicity was not observed after ACY-1215 treatment or the control groups (Figure 6E). We further analyzed the tumor cell proliferation marker Ki-67 to evaluate the drug efficacy in the tumor tissues. Compared with the vehicle group, the expression of Ki-67 was lower in the group treated with ACY-1215 (Figure 6F). Together, these findings indicate that ACY-1215 has therapeutic efficacy *in vivo*.

Discussion

Our findings demonstrated that an accumulation of acetylated GRP78 by HDAC6 inhibition is a potential target for an anti-tumor effect in CCA. This study showed that: 1) Acetylation of GRP78 by ACY-1215 increased, which led to suppression of translocation of GRP78 to the cell surface. 2) ACY-1215 inhibited proliferation by decreasing p-AKT (Ser473) and induced apoptosis *via* AKT-Bad signaling. 3) Knockdown of HDAC6 suppressed cell growth rate *via* decline in cs-GRP78. These data suggest that HDAC6 has a crucial a role in modifying GRP78 in CCA.

Previous studies have demonstrated the anti-tumor effect of pan-HDAC inhibitors, including vorinostat, TSA, VPA, and CG200745, in CCA cell lines (2-4). We also found that the proliferation of CCA cell line was suppressed by SAHA (Figure S1). However, since it has been reported that HDAC6 and its substrates were closely associated with cancer (23-25), we specifically focused on the role of HDAC6, and not all HDACs in CCA biology.

To investigate their roles and the relationship between HDAC6 and GRP78, we treated CCA cell lines with ACY-1215. In general, it is well-known that HDAC6 inhibition induces ER stress through the failure to clear misfolded proteins (26). However, the level of ubiquitin, a general ER-stress pattern, also did not change, while ACY-1215 induced the activation of ER chaperones GRP78 and phospho-PERK (Figure 3). With these observations, we suggested that the phospho-PERK might act as a responder to alleviate ER stress.

Among the ER chaperones, GRP78 is known to be a substrate of HDAC6 (7, 19). Actually, because cancer cells undergo prolonged ER stress, we considered whether GRP78 has a crucial role in CCA survival. It has been reported that ER stress-induced GRP78 translocation to the plasma membrane contributes to the survival of cancer (10, 15, 16). The GRP78 translocation mechanism involves a KDEL motif at the C-terminus of GRP78, which retrieves GRP78 from the Golgi apparatus to the ER *via* the KDEL receptor (8, 10). In effect, in a solid tumor under prolonged ER stress, the

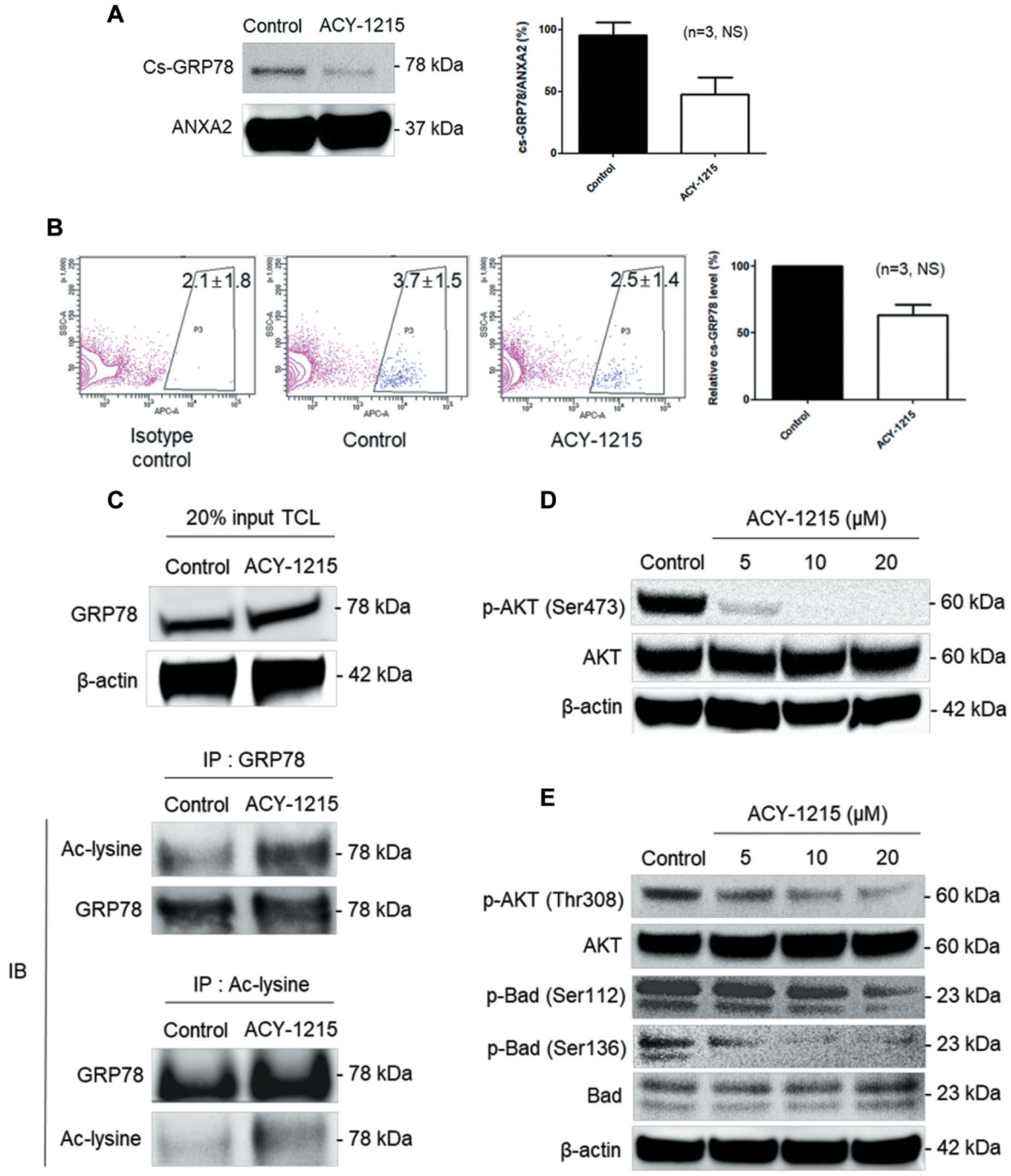

Figure 4. *ACY-1215 suppresses translocation of GRP78 to the cell surface via GRP78 acetylation, which affects proliferation and apoptosis via AKT/Bad signaling. (A) The TFK-1 cells were cultured with ACY-1215 at 10 μM for 24 h. Through the biotinylation assay, we labeled and purified the GRP78 located on the plasma membrane and detected the GRP78 via western blot analysis. (B) TFK-1 cells were either untreated (Control) or treated with 10 μM ACY-1215 for 24 h. Cell surface GRP78 were measured by FACS (Pink dots, Isotype control; Blue dots, anti-GRP78 antibody). Relative cell surface-GRP78 level in either untreated (Control) or treated cells with 10 μM ACY-1215 for 24 h (n=3). (C) TFK-1 cells were either untreated (Control) or treated with 10 μM ACY-1215 for 24 h. Subsequently, the lysates from the cell pellets were immunoprecipitated with anti-GRP78 antibody and anti-acetyl-lysine antibody, respectively, and immunoblotted for acetyl-lysine and GRP78, respectively. (D) Following ACY-1215 treatment at the indicated concentrations (5, 10 and 20 μM) for 24 h, p-AKT (Ser473) levels were detected by western blot. p-AKT (Ser473) related to the proliferation of cancer cells. (E) TFK-1 cells were treated with ACY-1215 at the indicated concentrations (5, 10 and 20 μM) for 24 h. Western blot shows the levels of p-AKT (Thr308), AKT, p-Bad (Ser112), p-Bad (Ser136), Bad and B-actin. p-AKT (Thr308) related to the blockade of apoptosis via Bad phosphorylation. All the experiments were performed three times.*

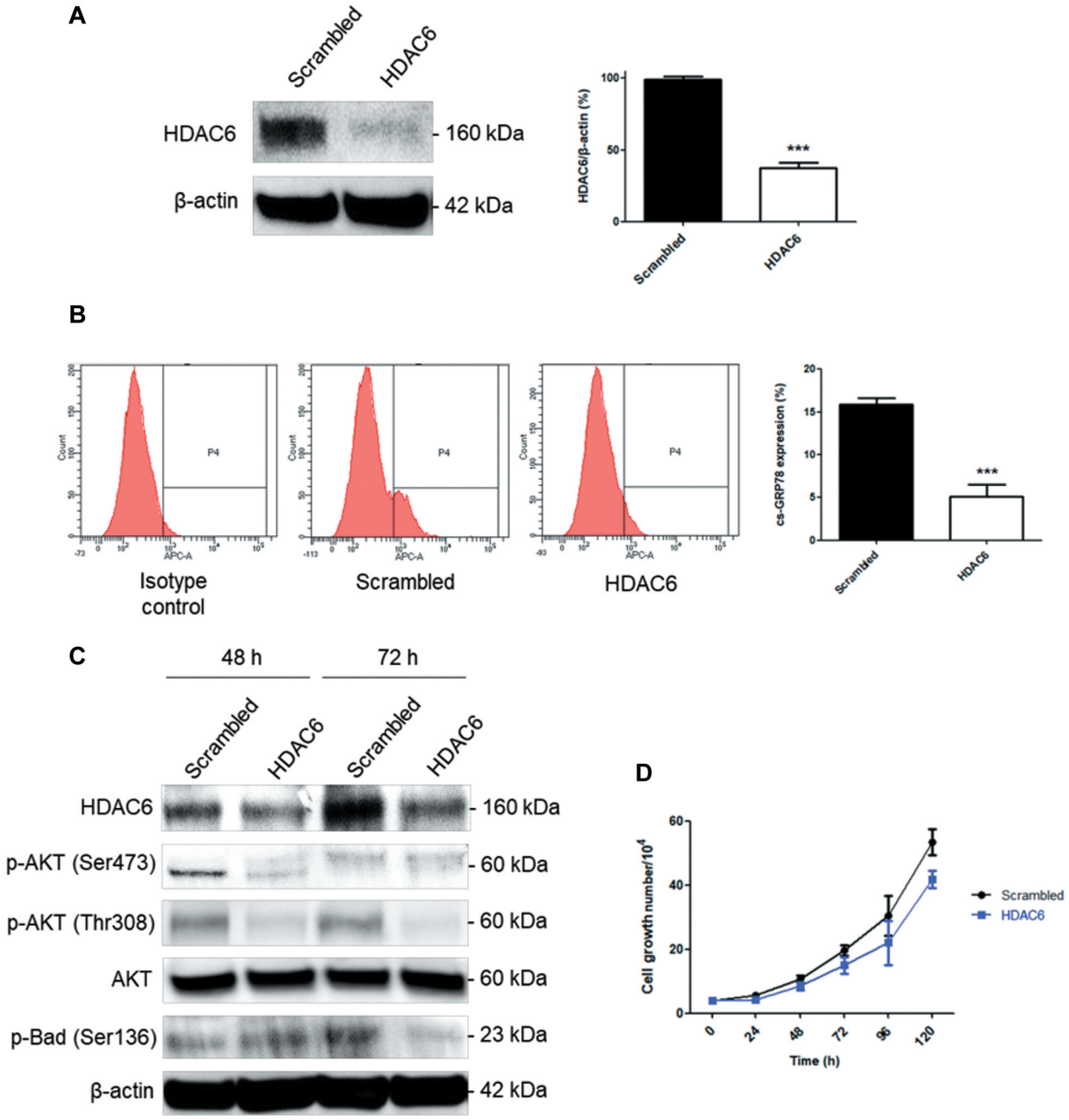

Figure 5. *The effects of HDAC6 knockdown on CCA cell proliferation and the protein expression levels of AKT/Bad. (A) The knockdown efficiency of HDAC6 siRNA was evaluated in TFK-1 cells. TFK-1 cells were transfected with 10 nM siRNA specifically targeting HDAC6, or scramble siRNA, and the siRNA-depletion efficiency was detected after 48 h using the indicated antibodies by western blotting. (B) At 48 h post-transfection, cell surface GRP78 proteins were measured by FACS. (C) The cells were transfected with 10 nM of the indicated siRNA for 48, and 72 h. HDAC6, p-AKT (Ser473), p-AKT (Thr308), AKT, and p-Bad (Ser136) were analyzed by western blotting. (D) Following siRNA-mediated knockdown, live cells were counted in a hemocytometer at 24 h intervals. All data were analyzed by two-tailed student's t-test, n=3. *p<0.05, ***p<0.001.*

total amount of GRP78 exceeds the KDEL binding capacity of the KDEL receptor, and only some of the GRP78 is retrieved to the ER. The rest of the GRP78 translocates to the cell surface (8, 27).

Recent studies have reported that GRP78, has critical roles in cancer progression and highlighted a potential target for cancer therapy (16-18, 21, 22). Treatment with the anti-GRP78 antibody MAb159, which specifically recognizes

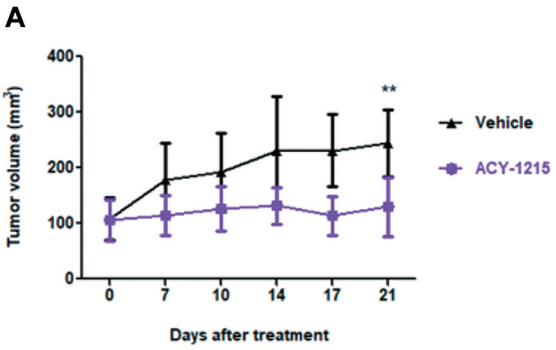

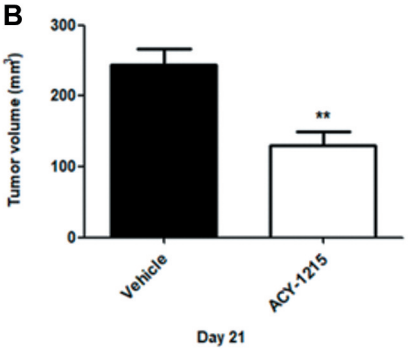

C

Tumor volume (Ave±SD, mm³)						
Days after treatment	0	7	10	14	17	21
Vehicel	108.3±37.8	179.1±65.2	191.7±71.5	230±97.9	231.3±65.9	244.7±59.6
ACY-1215	106±37	114.6±35.8	127±40	131.5±33.3	114.2±34.8	130.1±53.1

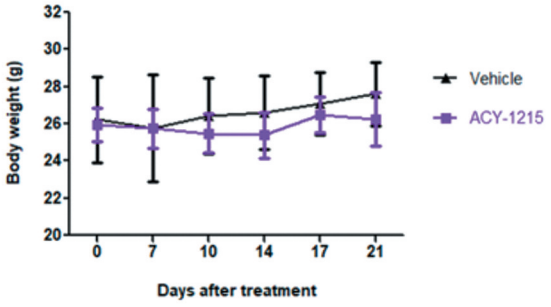

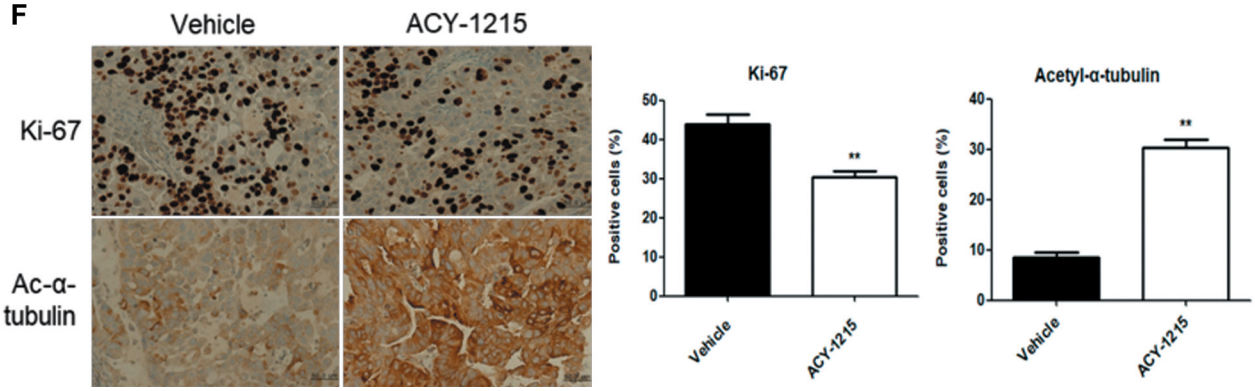

Figure 6. *HDAC6 inhibition suppresses tumor growth in cholangiocarcinoma (CCA) xenograft model. A total of 5×10⁶ TFK-1 cells were implanted into the flank of BALB/c nude mouse. When average tumor volume reached 100 mm³, ACY-1215 was administered via intraperitoneal injection (50 mg/kg) in the treatment group (n=7) 5 days a week for 3 weeks. Mice in the vehicle group (n=7) were treated with 5% DMSO + 45% PEG-400 + 50% ddH_2O (A) Time course of tumor growth in mice with or without ACY-1215 treatment. (B) After 21 days of treatment, tumor growth inhibition was 46% by ACY-1215. (**p<0.001). (C) Table of average tumor volume. (D) Mice after 28 days of treatment. (E) The body weight of mice after drug treatment up to day 76. (F) Immunohistochemical expression of Ki-67 and Ac-α-tubulin. A representative immunohistochemical (IHC) staining of tumor tissues with Ki-67 and Ac-α-tubulin. Quantification analysis of IHC staining of Ki-67 and Ac-α-tubulin (scale bar=100 μm, 40× magnification, **p<0.001, n=3 for each).*

surface GRP78, suppressed tumor growth *in vitro* and *in vivo* (16). The BOLD-100-001 phase Ib clinical study using BOLD-100 in combination with FOLFOX (5-fluorouracil, leucovorin, oxaliplatin) is ongoing. BOLD-100 reduces the expression of GRP78 in cancer cells.

In effect, our data demonstrated that the expression level of cs-GRP78 on the plasma membrane decreased and the level of acetylation on GRP78 increased by treatment with ACY-1215 (Figure 4). Liu et al. have reported that cs-GRP78 regulated PI3K/AKT signaling upstream *via* the interaction of cs-GRP78 with p85, a subunit of PI3K (16). AKT signaling regulates both proliferation and apoptosis according to the site of phosphorylation on AKT. Because cs-GRP78 acts as an α2-macroglobulin signaling receptor and interacts with PI3K, we looked for any alterations of the PI3K/AKT pathway, especially the phosphorylation sites of AKT, under ACY-1215 treatment. As expected, our findings showed alterations in AKT signaling. Both the proliferation signaling (Ser473 of AKT) and the anti-apoptotic signaling (Thr308 of AKT) were decreased (Figure 5A). These alterations on AKT affected BAD, a pro-apoptotic protein. Phosphorylation of BAD by AKT, known as the main kinase regulating BAD, induces its sequestration from the mitochondria, resulting in a blockade of apoptosis (28).

HDAC6 has been shown to have a role in CCA cell proliferation, and knockdown of HDAC6 decreased cell proliferation and anchorage-independent growth in CCA (5). Consistent with this observation, our data have shown that HDAC6 down-regulation by siRNA targeting HDAC6 causes a decline in CCA cell proliferation and activation of apoptosis.

Combining molecular targeted agents has been considered as a potential therapeutic strategy (29). Our findings suggest that PI3K/AKT signaling can be targeted to enhance the anti-tumor effects of HDAC6 inhibition. It has been reported that there is a synergic effect between HDAC and PI3K inhibition in cancer cell death (30), but the involvement of cs-GRP78 remains unclear. The combination of an HDAC6 inhibitor with a PI3K/AKT inhibitor is one potential strategy to overcome HDAC6 inhibitor resistance.

In conclusion, our results suggest that there is an association between HDAC6 and GRP78 on the plasma membrane, which promotes CCA growth and survival. We showed that blockade of GRP78 translocation to the plasma membrane *via* an increase in acetylated GRP78 caused by HDAC6 inhibition suppressed tumor growth and induced cell death of CCA *in vitro* and *in vivo*. Therefore, HDAC6 inhibitors could be a potential therapeutic approach to CCA.

Supplementary Material

Figure S1 is available at: https://zenodo.org/record/5712124#.YZcsAGBByUk

Conflicts of Interest

The Authors declare no potential conflicts of interest in relation to this study.

Authors' Contributions

Conception and design: CK, SL, CY, KPK; Development of methodology: CK, SL, DK, DSL; Experimental studies: CK, SL, DK, DSL; Analysis and interpretation of data: CK, SL, EL; Writing of the manuscript: CK, SL, CY, KPK; Technical support: CK, SL, DK, DSL; Review, and/or revision of the manuscript: CK, SL, CY, KPK; Study supervision: KPK; Approval of the manuscript: All Authors.

Acknowledgements

The Authors thank Dr. Seung-Mo Hong, Department of Pathology, Asan Medical Center for analysis of IHC data. The Authors also thank the core facilities of Comparative Pathology Core, Flowcytometry Core, Clinical Proteomics Core, Laboratory of Animal Research at the ConveRgence mEDIcine research cenTer (CREDIT), Asan Medical Center for the use of their shared equipment, services and expertise.

Funding

This research was supported by a grant from the Korea Health Technology R&D Project through the Korea Health Industry Development Institute (KHIDI), funded by the Ministry of Health & Welfare, Republic of Korea (grant number: HI18C2383).

References

1 Valle J, Wasan H, Palmer DH, Cunningham D, Anthoney A, Maraveyas A, Madhusudan S, Iveson T, Hughes S, Pereira SP, Roughton M, Bridgewater J and ABC-02 Trial Investigators: Cisplatin plus gemcitabine *versus* gemcitabine for biliary tract cancer. N Engl J Med *362(14)*: 1273-1281, 2010. PMID: 20375404. DOI: 10.1056/NEJMoa0908721

2 Sakamoto T, Kobayashi S, Yamada D, Nagano H, Tomokuni A, Tomimaru Y, Noda T, Gotoh K, Asaoka T, Wada H, Kawamoto K, Marubashi S, Eguchi H, Doki Y and Mori M: A histone deacetylase inhibitor suppresses epithelial-mesenchymal transition and attenuates chemoresistance in biliary tract cancer. PLoS One *11(1)*: e0145985, 2016. PMID: 26726879. DOI: 10.1371/journal.pone.0145985

3 Wang JH, Lee EJ, Ji M and Park SM: HDAC inhibitors, trichostatin A and valproic acid, increase E cadherin and vimentin expression but inhibit migration and invasion of cholangiocarcinoma cells. Oncol Rep *40(1)*: 346-354, 2018. PMID: 29767267. DOI: 10.3892/or.2018.6441

4 Jung DE, Park SB, Kim K, Kim C and Song SY: CG200745, an HDAC inhibitor, induces anti-tumour effects in cholangiocarcinoma cell lines *via* miRNAs targeting the Hippo pathway. Sci Rep *7(1)*: 10921, 2017. PMID: 28883618. DOI: 10.1038/s41598-017-11094-3

5 Gradilone SA, Radtke BN, Bogert PS, Huang BQ, Gajdos GB and LaRusso NF: HDAC6 inhibition restores ciliary expression and decreases tumor growth. Cancer Res *73(7)*: 2259-2270, 2013. PMID: 23370327. DOI: 10.1158/0008-5472.CAN-12-2938

6 Li T, Zhang C, Hassan S, Liu X, Song F, Chen K, Zhang W and Yang J: Histone deacetylase 6 in cancer. J Hematol Oncol *11(1)*: 111, 2018. PMID: 30176876. DOI: 10.1186/s13045-018-0654-9

7 Li Z, Zhuang M, Zhang L, Zheng X, Yang P and Li Z: Acetylation modification regulates GRP78 secretion in colon cancer cells. Sci Rep *6*: 30406, 2016. PMID: 27460191. DOI: 10.1038/srep30406

8 Ni M, Zhang Y and Lee AS: Beyond the endoplasmic reticulum: atypical GRP78 in cell viability, signalling and therapeutic targeting. Biochem J *434(2)*: 181-188, 2011. PMID: 21309747. DOI: 10.1042/BJ20101569

9 Kim H, Bhattacharya A and Qi L: Endoplasmic reticulum quality control in cancer: Friend or foe. Semin Cancer Biol *33*: 25-33, 2015. PMID: 25794824. DOI: 10.1016/j.semcancer.2015.02.003

10 Tsai YL, Zhang Y, Tseng CC, Stanciauskas R, Pinaud F and Lee AS: Characterization and mechanism of stress-induced translocation of 78-kilodalton glucose-regulated protein (GRP78) to the cell surface. J Biol Chem *290(13)*: 8049-8064, 2015. PMID: 25673690. DOI: 10.1074/jbc.M114.618736

11 Ni M, Zhou H, Wey S, Baumeister P and Lee AS: Regulation of PERK signaling and leukemic cell survival by a novel cytosolic isoform of the UPR regulator GRP78/BiP. PLoS One 4(8): e6868, 2009. PMID: 19718440. DOI: 10.1371/journal.pone.0006868

12 Huang SP, Chen JC, Wu CC, Chen CT, Tang NY, Ho YT, Lo C, Lin JP, Chung JG and Lin JG: Capsaicin-induced apoptosis in human hepatoma HepG2 cells. Anticancer Res 29(1): 165-174, 2009. PMID: 19331147.

13 Fu R, Yang P, Wu HL, Li ZW and Li ZY: GRP78 secreted by colon cancer cells facilitates cell proliferation *via* PI3K/Akt signaling. Asian Pac J Cancer Prev 15(17): 7245-7249, 2014. PMID: 25227822. DOI: 10.7314/apjcp.2014.15.17.7245

14 Li R, Yanjiao G, Wubin H, Yue W, Jianhua H, Huachuan Z, Rongjian S and Zhidong L: Secreted GRP78 activates EGFR-SRC-STAT3 signaling and confers the resistance to sorafeinib in HCC cells. Oncotarget *8(12)*: 19354-19364, 2017. PMID: 28423613. DOI: 10.18632/oncotarget.15223

15 Li Z and Li Z: Glucose regulated protein 78: a critical link between tumor microenvironment and cancer hallmarks. Biochim Biophys Acta *1826(1)*: 13-22, 2012. PMID: 22426159. DOI: 10.1016/j.bbcan.2012.02.001

16 Liu R, Li X, Gao W, Zhou Y, Wey S, Mitra SK, Krasnoperov V, Dong D, Liu S, Li D, Zhu G, Louie S, Conti PS, Li Z, Lee AS and Gill PS: Monoclonal antibody against cell surface GRP78 as a novel agent in suppressing PI3K/AKT signaling, tumor growth, and metastasis. Clin Cancer Res *19(24)*: 6802-6811, 2013. PMID: 24048331. DOI: 10.1158/1078-0432.CCR-13-1106

17 Misra UK, Deedwania R and Pizzo SV: Binding of activated alpha2-macroglobulin to its cell surface receptor GRP78 in 1-LN prostate cancer cells regulates PAK-2-dependent activation of LIMK. J Biol Chem *280(28)*: 26278-26286, 2005. PMID: 15908432. DOI: 10.1074/jbc.M414467200

18 Yao X, Liu H, Zhang X, Zhang L, Li X, Wang C and Sun S: Cell surface GRP78 accelerated breast cancer cell proliferation and migration by activating STAT3. PLoS One *10(5)*: e0125634, 2015. PMID: 25973748. DOI: 10.1371/journal.pone.0125634

19 Baumeister P, Dong D, Fu Y and Lee AS: Transcriptional induction of GRP78/BiP by histone deacetylase inhibitors and resistance to histone deacetylase inhibitor-induced apoptosis. Mol Cancer Ther *8(5)*: 1086-1094, 2009. PMID: 19417144. DOI: 10.1158/1535-7163.MCT-08-1166

20 Peng U, Wang Z, Pei S, Ou Y, Hu P, Liu W and Song J: ACY-1215 accelerates vemurafenib induced cell death of BRAF-mutant melanoma cells *via* induction of ER stress and inhibition of ERK activation. Oncol Rep *37(2)*: 1270-1276, 2017. PMID: 28035401. DOI: 10.3892/or.2016.5340

21 Li Z, Zhang L, Zhao Y, Li H, Xiao H, Fu R, Zhao C, Wu H and Li Z: Cell-surface GRP78 facilitates colorectal cancer cell migration and invasion. Int J Biochem Cell Biol *45(5)*: 987-994, 2013. PMID: 23485528. DOI: 10.1016/j.biocel.2013.02.002

22 Misra UK, Deedwania R and Pizzo SV: Activation and cross-talk between Akt, NF-kappaB, and unfolded protein response signaling in 1-LN prostate cancer cells consequent to ligation of cell surface-associated GRP78. J Biol Chem *281(19)*: 13694-13707, 2006. PMID: 16543232. DOI: 10.1074/jbc.M511694200

23 Saji S, Kawakami M, Hayashi S, Yoshida N, Hirose M, Horiguchi S, Itoh A, Funata N, Schreiber SL, Yoshida M and Toi M: Significance of HDAC6 regulation *via* estrogen signaling for cell motility and prognosis in estrogen receptor-positive breast cancer. Oncogene *24(28)*: 4531-4539, 2005. PMID: 15806142. DOI: 10.1038/sj.onc.1208646

24 Tsutsumi S, Beebe K and Neckers L: Impact of heat-shock protein 90 on cancer metastasis. Future Oncol *5(5)*: 679-688, 2009. PMID: 19519207. DOI: 10.2217/fon.09.30

25 Ding G, Liu HD, Huang Q, Liang HX, Ding ZH, Liao ZJ and Huang G: HDAC6 promotes hepatocellular carcinoma progression by inhibiting P53 transcriptional activity. FEBS Lett *587(7)*: 880-886, 2013. PMID: 23402884. DOI: 10.1016/j.febslet.2013.02.001

26 Feng Y, Huang R, Guo F, Liang Y, Xiang J, Lei S, Shi M, Li L, Liu J, Feng Y, Ma L and Fu P: Selective histone deacetylase 6 inhibitor 23BB alleviated rhabdomyolysis-induced acute kidney injury by regulating endoplasmic reticulum stress and apoptosis. Front Pharmacol *9*: 274, 2018. PMID: 29632491. DOI: 10.3389/fphar.2018.00274

27 Zhang Y, Liu R, Ni M, Gill P and Lee AS: Cell surface relocalization of the endoplasmic reticulum chaperone and unfolded protein response regulator GRP78/BiP. J Biol Chem *285(20)*: 15065-15075, 2010. PMID: 20208072. DOI: 10.1074/jbc.M109.087445

28 Datta SR, Dudek H, Tao X, Masters S, Fu H, Gotoh Y and Greenberg ME: Akt phosphorylation of BAD couples survival signals to the cell-intrinsic death machinery. Cell *91(2)*: 231-241, 1997. PMID: 9346240. DOI: 10.1016/s0092-8674(00)80405-5

29 Soria JC, Blay JY, Spano JP, Pivot X, Coscas Y and Khayat D: Added value of molecular targeted agents in oncology. Ann Oncol *22(8)*: 1703-1716, 2011. PMID: 21300696. DOI: 10.1093/annonc/mdq675

30 Sun K, Atoyan R, Borek MA, Dellarocca S, Samson ME, Ma AW, Xu GX, Patterson T, Tuck DP, Viner JL, Fattaey A and Wang J: Dual HDAC and PI3K inhibitor CUDC-907 downregulates MYC and suppresses growth of MYC-dependent cancers. Mol Cancer Ther *16(2)*: 285-299, 2017. PMID: 27980108. DOI: 10.1158/1535-7163.MCT-16-0390

Received August 27, 2021
Revised November 17, 2021
Accepted November 19, 2021